ISSN 0252-1075

Research Report No.RR-061

Contributions from

Indian Institute of Tropical Meteorology

Identification of Self-organized Criticality in the Interannual Variability of Global Surface Temperature

By

A.M. Selvam, and M. Radhamani

PUNE-411 008
INDIA

OCTOBER 1994

Identification of Self-organized criticality in the interannual variability of global surface temperature

A.M. Selvam and M. Radhamani
Indian Institute of Tropical Meteorology,
Pune 411 008, India

Abstract

Continuous periodogram analyses of sets of 25-years hemispheric surface temperature time series show that the power spectra follow the universal inverse power law form of the statistical normal distribution. Inverse power law form for the power spectra of temporal fluctuations is ubiquitous to real world dynamical systems and is a signature of self-organized criticality. A recently developed cell dynamical system model for atmospheric flows predicts the observed universal spectrum as intrinsic to quantum-like mechanics governing flow dynamics. Such unique quantification for self-organized criticality implies predictability of the total pattern of fluctuations over a period of time. Universal spectrum for interannual variability rules out indefinite linear secular trends in surface temperature.

1. Introduction

Long-range spatiotemporal correlations manifested as the fractal geometry to the spatial pattern (spatial correlations) concomitant with inverse power law form for the power spectrum of temperal fluctuations (temporal correlations) are ubiquitous to spatially extended dynamical systems in nature and are recently identified as signatures of self-organized criticality (Bak, Tang and Wiesenfeld, 1988). Self-organized criticality in atmospheric flows is seen as the fractal geometry to the global cloud cover pattern and inverse power law form for atmospheric eddy energy spectrum documented and discussed by Lovejoy and Schertzer (1986) and Tessier et al (1993). The physics of self-organized criticality is not yet identified. A recently developed cell dynamical system model for atmospheric flows (Mary Selvam, 1990; Mary Selvam et al., 1992; Mary Selvam, 1993; Selvam and Radhamani, 1993; Selvam and Joshi, 1994) predicts the observed self-organized criticality as intrinsic to quantum-like mechanics governing flow dynamics. Such unique quantification for self-organized criticality implies predictability of the total pattern of fluctuations.

Continuous periodogram analyses of sets of 25-years hemispheric annual mean surface temperature time series show that the power spectra follow the universal inverse power law form of the statistical normal distribution in agreement with model predictions.

2. Cell Dynamical System Model

The model concepts have been discussed in detail in earllier publications (Mary Selvam, 1990; Mary Selvam et al., 1992; Selvam and Radhamani, 1993). The model predictions are as follows: (1) The power spectrum of temporal fluctuations represents the statistical normal distribution with the percentage contribution to total variance equal to the percentage probability of occurrence corresponding to the normalised standard deviation t given as

$$t = (\mathrm{Log}\ L/\mathrm{Log}\ T_{50})-1 \qquad (1)$$

where L is the period in years and T_{50} correspond to the period up to which the cumulative percentage contribution to total variance is equal to 50. (2) The atmospheric circulation pattern consists of an overall logarithmic spiral trajectory with the quasiperiodic Penrose tiling pattern for the internal structure. Such an atmospheric eddy continuum (spiral flow structure) has embedded dominant wavebands whose peak periodicities P_n are given as

$$P_n = T(2+\tau)\tau^n \qquad (2)$$

where τ is the golden mean equal to $(1+\sqrt{5})/2$ (=1.618) and the exponent n ranges from zero to positive and negative integer value. T is the primary perturbation time period equal to the annual (summer to winter) cycle of solar heating in the present study. The spiral-like structure is seen as a progressive increase of phase angle with increase in period. The bandwidth of dominant wavebands increase with increase in period length.

The above model predictions are in agreement with continuous periodogram spectral analysis of annual mean hemispheric surface temperature time series as shown in the following sections.

3. Data and Analysis

Annual mean hemispheric (North and South) surface temperature anomalies with respect to 1951-80 (Parker and Jones, 1991) for the period 1866-1990 was used for the study. Five sets of successive 25-year time series (1866-1890, 1891-1915, 1916-1940, 1941-1965 and 1966-1990) were subjected to quasicontinuous periodogram spectral analysis (Jenkinson, 1977). The cumulative percentage contribution to total variance was computed starting from the high frequency side of the spectrum. The period T_{50} at which 50% contribution to total variance occurs is taken as reference and the normalised standard deviation t_m values are computed (Eq.2) as

$$t_m = (\log m/\log T_{50}) - 1$$

The cumulative percentage contribution to total variance and the corresponding t values are plotted in Fig.1 as continuous and dotted respectively for the Northern and Southern hemispheric surface temperatures. The cumulative normal probability density distribution corresponding to the normalised standard deviation t values are shown as crosses in Fig.1. It is seen that the cumulative percentage contribution to total variance closely follows the cumulative normal probability density distribution. The "goodness of fit" of the power spectra with the normal distribution was tested using the standard statistical chi-square test. All the spectra follow normal distribution characteristics except for one marked ns in Fig.1.

The percentage contribution to total variance and phase angle for dominant eddies (percentage contribution to total variance greater than .01) and the cumulative percentage contribution to total variance for periodicities 2 to 30 years are plotted in Fig.2 for the Northern and Southern Hemispheric surface temperature for the five sets of time series. It is seen that dominant periodicities have broadband structure, the bandwidth increasing with period length. Further, there is a smooth uniform rotation of the phase angle with increasing period length within a waveband and from one waveband to the next implying spiral-like continuous structure for the eddy continuum. The above result implies long-range temporal correlations and is consistent with model prediction of self-organized criticality.

Table 1 gives the following periodogram estimates for the Northern and Southern hemisphere surface temperature time series data sets. (1) Mean and standard deviation of the time series. (2) The period T_{50}, up to which the cumulative percentage contribution to total variance is equal to 50. (3) Peak periodicities in the waveband with normalised variance equal to or more than one. Asterisk (*) indicates statistical significance equal to or less than 5%.

4. Discussion and Conclusion

It is seen (Table 1) that peak periodicities in dominant wavebands are consistent with model predicted (Eq.2) periodicities (years) 2.2, 3.6, 5.8, 9.5, 15.3, 24.8 respectively for n ranging from -1 to 4. These periodicities correspond to the well documented atmospheric cycles :(1) The quasibiennial oscillation (QBO) of 2.2 years, (2) the El Nino/Southern Oscillation (ENSO) of 3-7 years and (3) interdecadal (> 9 years) oscillations.

The important conclusion of the present study is the identification of the universal inverse power law form of the statistical normal distribution for the power spectrum of interannual variability of atmospheric flows. Global COADS (Comprehensive Ocean Atmosphere Data Set) surface (air and sea) temperature time series also exhibit the universal spectrum (Selvam and Joshi 1994). Universal spectrum rules out linear secular trends in global surface temperature. Energy input to the atmospheric eddy continuum from green-house gas warming effect will result in enhancement of fine structure of the universal spectrum, i.e. of intensification of the quasibiennial and high frequency component of ENSO cycle.

Acknowledgement

The authors are grateful to Dr. A.S.R. Murty for his keen interest and encouragement during the course of the study. Thanks are due to Mrs. A.A. Ursekar for typing the manuscript.

References

Bak, P.C., C. Tang and K. Wiesenfeld, 1988: Self-organized criticality. *Phy.Rev.* A**38**, 364-374,

Jenkinson, A.A., 1977: *A powerful elementary method of spectral analysis for use with monthly, seasonal or annual meteorological time series*. Met O 13 Branch Memorandum No.57, U.K. Meteorological Office, London, pp. 23.

Lovejoy, S., and D. Schertzer, 1986: Scale invariance, symmetries, fractals and stochastic simulations of atmospheric phenomena. *Bull.Amer.Meteor.Soc.* **67**, 21-32.

Mary Selvam, A., 1990 : Deterministic chaos, fractals and quantum-like mechanics in atmospheric flows. *Can.J.Phys.* **68**, 831-841.

Mary Selvam, A., J.S. Pethkar and M.K. Kulkarni, 1992: Signatures of a universal spectrum for atmospheric interannual variability in rainfall time series over the Indian region. *Int'l.J.Climatol.* **12**, 137-152.

Mary Selvam, A., 1993 : A universal spectrum for interannual variability of monsoon rainfall over India. *Adv.Atmos.Sci.* **10(2)**, 221-226.

Parker, D.E. and P.D. Jones, 1991 : Global warmth in 1990. *Weather* **46**, 302-310.

Selvam, A.M., and M. Radhamani, 1993 : *Identification of self-organized criticality in atmospheric total ozone variability*. IITM Research Report No. RR-057, pp.16.

Selvam, A.M., and R.R. Joshi, 1994 : Universl spectrum for interannual variability in COADS global air and sea surface temperatures. *Int'l.J.Climatol.* (Accepted).

Tessier, Y., S. Lovejoy and D. Schertzer, 1993 : Universal multifractals : Theory and observations for rain and clouds. *J. Appl.Meteor.* **32(2)**, 223-250.

Table 1 : Periodogram estimates.

Sr. No.	Period	Mean	Std. dev. (°C)	T_{50} (years)	Peak periodicities (years) in the wave-band with normalised variance greater than or equal to 1				
1.	1866-90								
	NH	-.21	.15	5.44	4.68	10.65			
	SH	-.21	.09	4.84	2.30	2.80	3.65	5.64	15.31
2.	1891-1915								
	NH	-.29	.14	8.70	2.97	4.81	8.60	16.88*	
	SH	-.24	.12	13.92	4.50	8.84	18.23		
3.	1916-1940								
	NH	-.10	.18	15.00	5.92	8.36	13.48		
	SH	-.16	.10	9.32	6.35	9.09	14.28		
4.	1941-1965								
	NH	.06	.12	5.17	2.74	4.79	8.40	15.26	
	SH	-.05	.12	4.90	2.00	4.31	8.45	15.72	
5.	1966-1990								
	NH	.05	.17	10.76	2.12	9.39			
	SH	.13	.14	13.28	2.55	3.63	4.82	8.69	13.45

* indicates significance at or less than 5% level.
NH Northern Hemisphere
SH Southern Hemisphere.

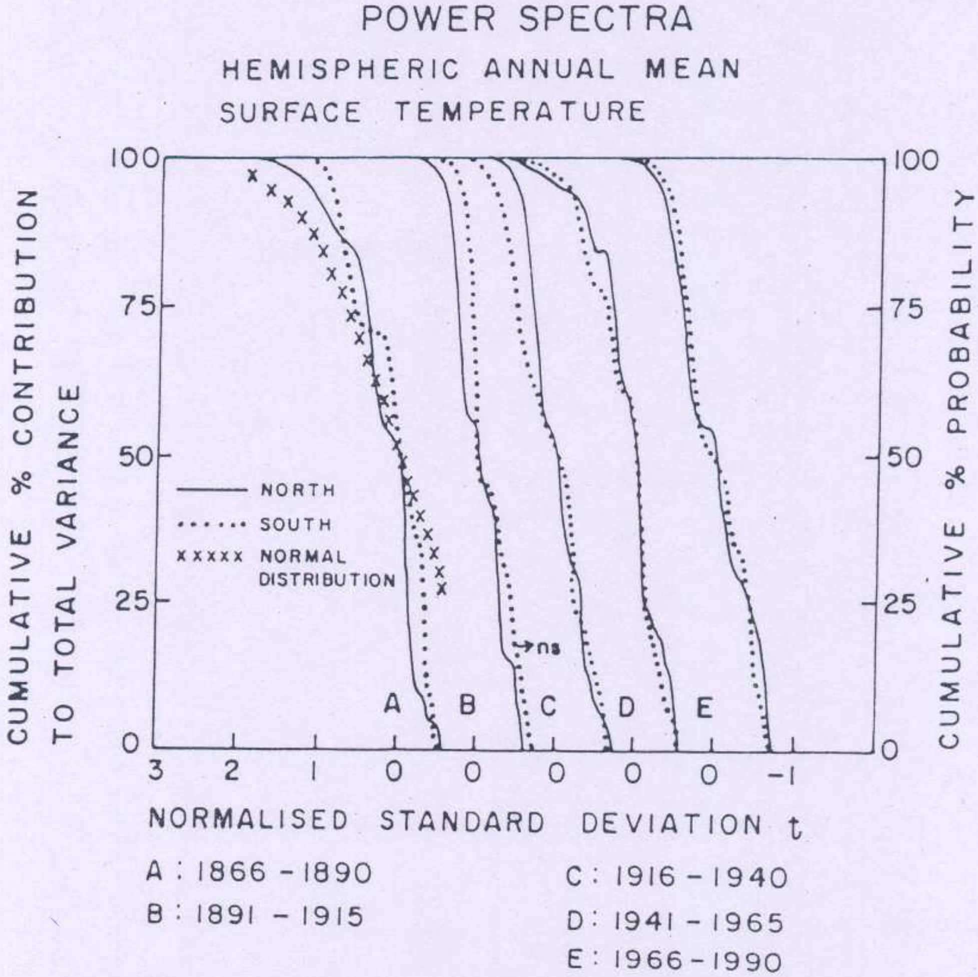

Figure 1 : Power spectra for the Northern and Southern Hemispheric surface temperature time series plotted as cumulative percentage contribution to total variance versus the normalised standard deviation t (see text).

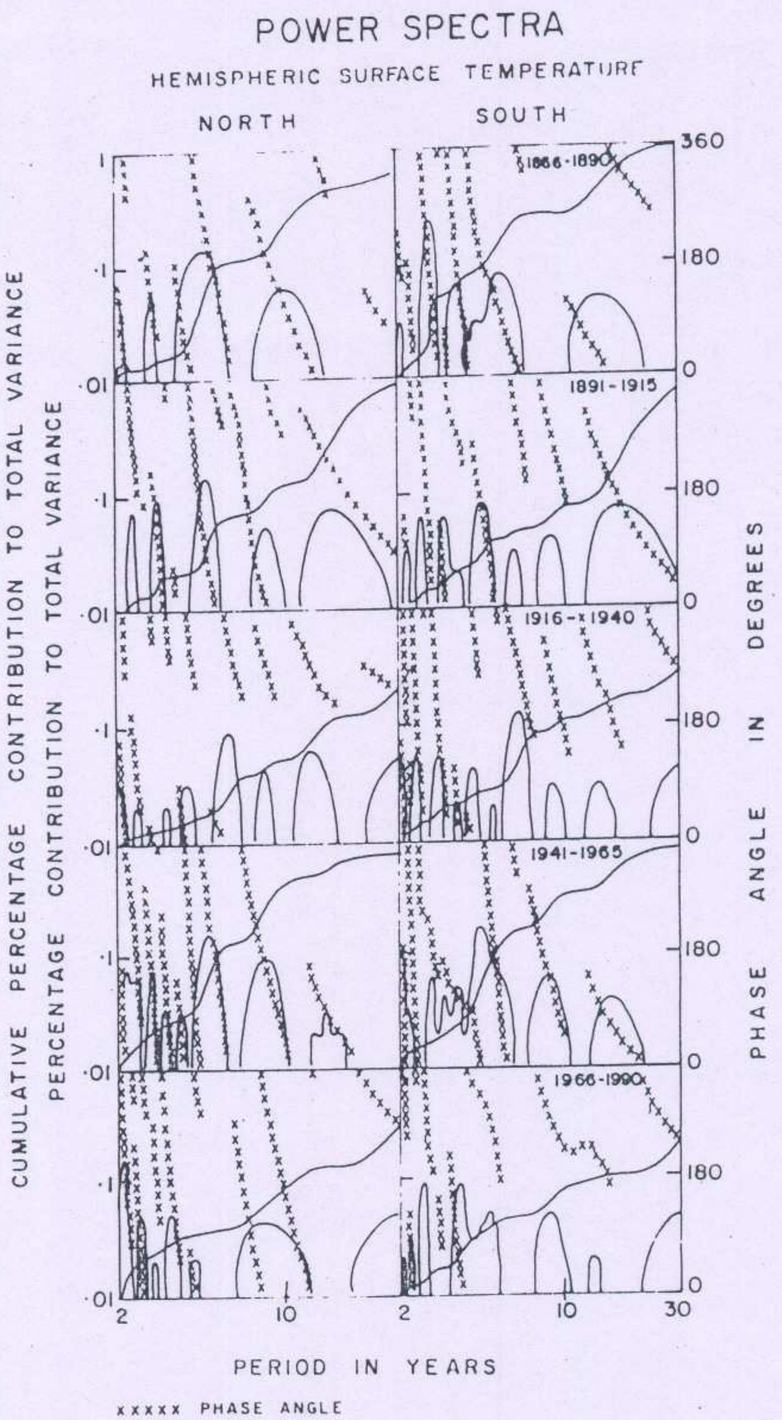

Figure 2 : Periodogram estimates of percentage contribution to total variance and phase for dominant eddies (% contribution to total variance > .01) and the cumulative percentage contribution to total variance corresponding to spectra shown in Figure 1. The logarithmic scale on the y-axis ranging from .01 to 1 refers to % contribution to total variance by dominant eddies. The cumulative percentage contribution to total variance shown as the continuous ascending line from left to right corresponds to y-axis scale range 0 to 100.